Volume 3
Number 12
December 2024
Pages 2387-2638

Digital Discovery

rsc.li/digitaldiscovery

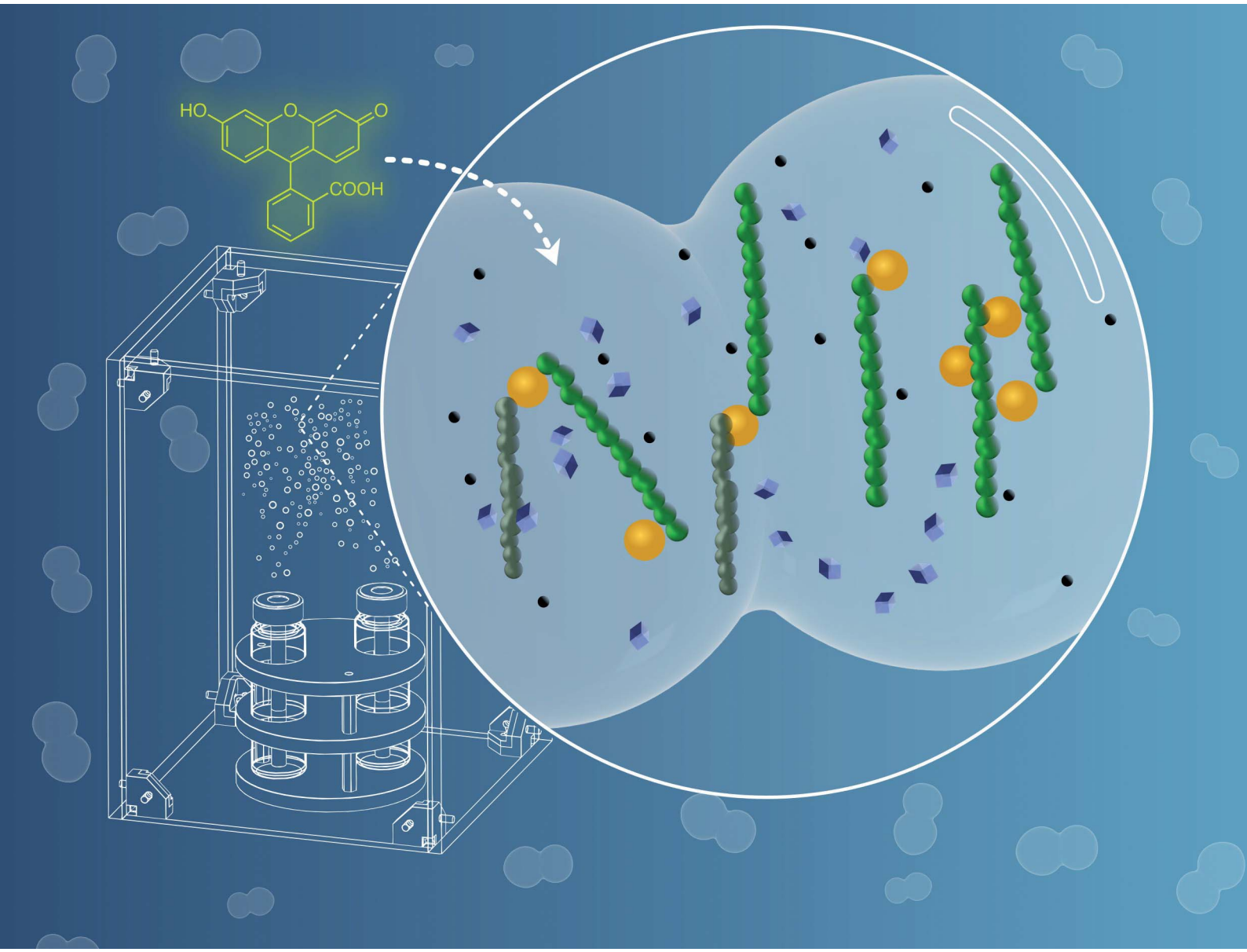

ISSN 2635-098X

ROYAL SOCIETY OF CHEMISTRY

PAPER

Luokun Zhang and S. Hessam M. Mehr
In situ synthesis within micron-sized hydrogel reactors created *via* programmable aerosol chemistry

Digital Discovery

ROYAL SOCIETY OF CHEMISTRY

PAPER

View Article Online
View Journal | View Issue

Cite this: *Digital Discovery*, 2024, **3**, 2424

In situ synthesis within micron-sized hydrogel reactors created *via* programmable aerosol chemistry†

Luokun Zhang and S. Hessam M. Mehr *

Recent progress in materials science and complex chemical systems has highlighted the critical role of containers in directing and modulating reactivity. Micron-sized reactors are especially attractive due to their significantly different surface/volume ratios compared to traditional laboratory glassware, while still providing high experimental throughput and being easily observable using optical microscopy. Despite their promise, there is a gap in adapting chemical synthesis protocols to work within microspheres. We demonstrate a programmable aerosol chemistry setup that automates the generation of calcium alginate microspheres and allows them to be used as micro-reactors for exploration of chemical reactivity. A range of reactions can be adapted for *in situ* synthesis within the forming microspheres by pre-loading the precursor solutions with solid and soluble reagents, exemplified by our preparation of Prussian blue and quinhydrone. The micro-reactors are permeable, allowing rapid uptake and release of small molecule reagents and products. Larger particles trapped within the calcium alginate matrix can also be released, triggered *via* rapid disassembly of the microspheres in response to calcium binders like EDTA. As our standard programmable apparatus is extensible to broad reagent types and reaction stoichiometries, we expect that its adoption will accelerate exploration of chemical reactivity and discovery within micro-reactors.

Received 25th May 2024
Accepted 13th October 2024

DOI: 10.1039/d4dd00139g

rsc.li/digitaldiscovery

Introduction

The concept of containment is central to all areas of chemistry, defining how chemicals and their reactions are observed and studied. Mixed reactants in a vessel have represented the smallest practical unit of reactivity, commonly achieved using familiar laboratory glassware in a research setting. With the advent of automation and the need for higher experimental throughout, new types of containers such as 96-well plates[1] have been devised to accommodate larger numbers of reactions simultaneously. Although innovations like optical tweezers and supramolecular structures[2–5] have made it possible to confine single molecules or nanoparticles,[6–9] for practical exploration of chemical reactivity, a containment length scale that accommodates an ensemble of reactant and solvent molecules is required, alongside sufficient throughput for scale-up. In this context, micron-sized reactors offer a vast throughput advantage whilst remaining adaptable to established laboratory workflows, Fig. 1A.[10,11]

Chemical containment on the micron scale can be accomplished using a range of techniques, including microfluidics[12,13] and self-assembly.[14] For use as micro-reactors, containers would ideally be synthesisable *in situ*, facilitating the inclusion of payloads (*e.g.* nanoparticles or proteins) instead of requiring their incorporation post-synthesis. Additionally, the ability to exchange species with the surrounding environment can enhance the micro-containers' versatility, enabling application as catalyst hosts,[15] sensors,[16] and in selective payload release.[17] Micron-scale confinement of reactions is also of profound interest for its influence on reaction kinetics and thermodynamics,[18,19] and for offering a transition between homogeneous and inhomogeneous reactivity for reactions in the millisecond–minute time scale, Fig. 1B. The influence of the hydrogel matrix itself is also relevant and has been used in the past to alter crystallisation of calcite[20] and metal–organic frameworks, inspired by its role in directing biomineralization in nature.[21]

Calcium alginate gel is an excellent basis for synthesising microreactors. Aqueous sodium alginate solutions can combine with calcium ions to form a biocompatible soft material made of calcium cross-linked strands of alginate. Its derivation from inexpensive and renewable algal feedstock, along with its straightforward synthesis and remarkable stability[22,25,26] underlies the widespread usage of calcium alginate in the food industry,[27] medicine and cosmetics,[28,29] and agriculture.[30] Despite extensive deployment, including the development of methodology for synthesising alginate microspheres,[31–33] the versatility of calcium alginate particles as chemical reactors has not been explored. Moreover, current protocols are largely reliant on microfluidics,[34] painstaking stepwise assembly of more complex composite structures,[35] or coacervates dependent

School of Chemistry, University of Glasgow, Advanced Research Centre, 11 Chapel Lane, Glasgow G11 6EW, UK. E-mail: Hessam.Mehr@glasgow.ac.uk

† Electronic supplementary information (ESI) available. See DOI: https://doi.org/10.1039/d4dd00139g

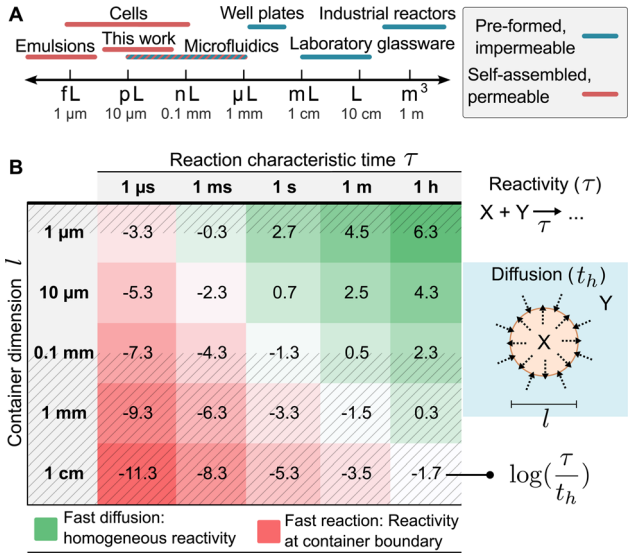

Fig. 1 Containment length scales and their potential impact on locus of reactivity. (A) Common containment modalities across volume regimes categorised by means of formation (pre-formed *versus* self-assembled) and permeability. (B) Transition from homogeneous (activation controlled) to inhomogeneous (diffusion controlled) reactivity with varying reaction characteristic time τ and container dimension l. Tabulated numbers show the logarithmic ratio of reaction (τ) and diffusion (t_h) time scales $\log\left(\frac{\tau}{t_h}\right)$, assuming mutually reactive species on opposite sides of a permeable hydrogel reactor with diffusion coefficient $D = 5.0 \times 10^{-10}$ m^2 s^{-1} (a representative value for small organic molecules in hydrogel matrix).[22–24] The dimension regime explored in this work is delineated as one order of magnitude around 10 μm.

on fine-tuned solution composition,[36] requiring significant adjustments for adoption in mainstream chemistry.

Aerosols have seen recent adoption in the fields of drug delivery,[37,38] air purification,[39] and printing technology[40] owing to the small size and high surface aera of their constituent microdroplets. These aerosol characteristics enable unique transport properties[41,42] and applications requiring an abundance of individual microscopic chemical packets.[41,43] In principle, aerosols provide an ideal pathway to accessing micron-sized containers, as many sources naturally emit particles in this size range.[11,44] Still, existing materials applications have largely overlooked the chemical versatility of aerosol particles, focusing on atomisation as a means of dispersion, for instance in the flame aerosol synthesis of inorganic nanoparticles.[45–47] Conversely, calcium alginate is ideally positioned for solution synthesis from sodium alginate microdroplets, attested to by previous work on aerosol synthesis of calcium alginate microcapsules.[48–50]

In this work, we demonstrate the aerosol synthesis of micron-sized soft chemical containers and their suitability as reaction containers.‡ Using a bespoke computer-controlled aerosol generator, we generated a mist of aqueous microdroplets containing dissolved sodium alginate along with any other reactants or solid payload. Upon precipitation into bulk solution containing Ca^{2+} ions, individual aerosol particles are transformed into hydrogel microspheres. Meanwhile, reagents included in the alginate droplets can react with those in the bulk solution, exemplified by the *in situ* synthesis of Prussian blue from $Na_4[Fe(CN)_6]$ and $FeCl_3$ in the aerosol and bulk solutions, respectively. Simultaneously, solid particles pre-loaded by dispersing in the alginate solution are encapsulated even though the microspheres remain permeable to small organic molecules, such as methylene blue or phenolphthalein. Both *in situ*-synthesised and pre-loaded guests can subsequently be liberated by a calcium sequestering agent like EDTA, providing a mechanism for chemically triggered payload release.

Results and discussion

Achieving *in* situ reactivity within micro-reactors firstly requires self-assembly of the reactor structures themselves, in this case microspheres of calcium alginate hydrogels, with concomitant combination of compounds involved in the contained reaction. Calcium alginate synthesis in particular relies on the mixing of separate Ca^{2+} and alginate solutions, each of which contain additional reactive compounds that participate in *in situ* reactivity upon contact. An aerosol-assisted methodology could therefore involve microdroplets of one reagent solution precipitating into a pool of the other (aerosol–bulk reactivity, Fig. 2A) or collisions between the respective solution microdroplets in an aerosol mixture (aerosol–aerosol reactivity, Fig. 2B).

Aerosol–bulk reactivity

Aqueous aerosol particles are subject to rapid ripening and eventual precipitation, at which point they can be captured within another bulk solution. With microdroplets of calcium chloride solution collected in a Petri dish containing alginate solution, the entire bulk solution was seen to increase in viscosity with further exposure to Ca^{2+} aerosol, eventually being transformed into a homogenous block of hydrogel. This observation is in line with the rapid diffusion of Ca^{2+} ions within the microdroplets into bulk alginate solution upon contact. On the other hand, when sodium alginate microdroplets are allowed to precipitate into bulk calcium chloride solution, the formation of colourless microspheres is readily verified *via* optical microscopy as 5–40 μm diameter spheres, Fig. 3A and B.

Initial attempts to visualise the resulting microspheres by addition of a dye to the sodium alginate solution — trialling methylene blue, fluorescein, and basic phenolphthalein — yielded colourless microspheres irrespective of dye concentration. The rapid loss of colour is evidence of dye diffusion into the surrounding solution, underlining the permeability of the soft microspheres towards small organic molecules. In contrast, using a pigment such as sumi carbon black ink resulted in particles that retained their colouration, rendering droplets

‡ In this context, 'soft' specifically refers to materials that can be easily deformed by external forces, such as hydrogels.

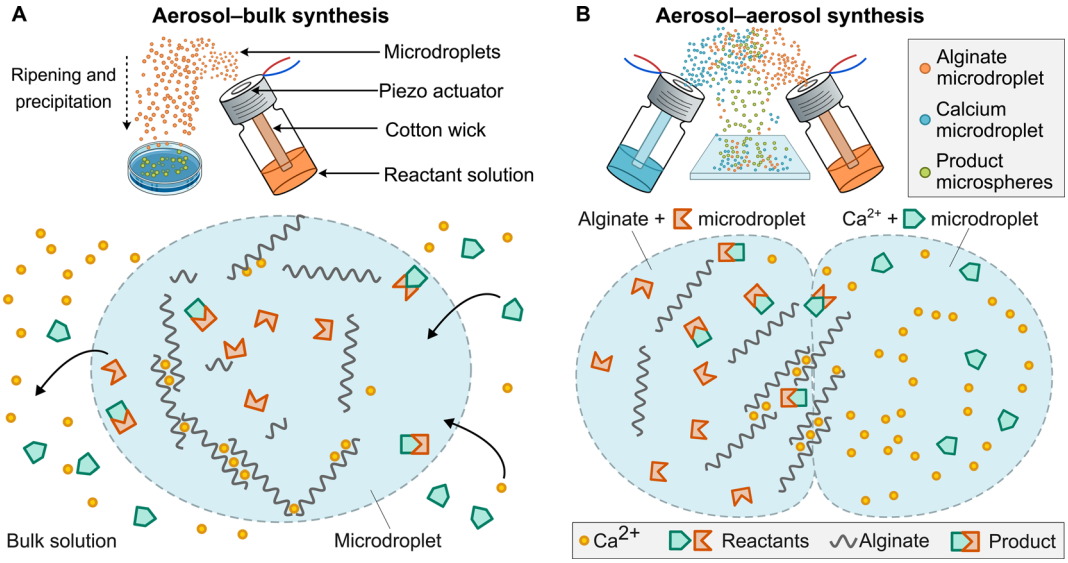

Fig. 2 Realisation of *in situ* reactivity within micro-reactors using aerosol–bulk or aerosol–aerosol routes. (A) In aerosol–bulk synthesis, reactivity occurs as sodium alginate-containing aerosol particles precipitate into bulk Ca^{2+} solution. (B) Aerosol–aerosol synthesis relies on the collision of alginate and Ca^{2+}, microdroplets each preloaded with reagents and aerosolised. Reactivity between the preloaded reagents occurs concomitantly with formation of calcium alginate microspheres as the two droplet types collide.

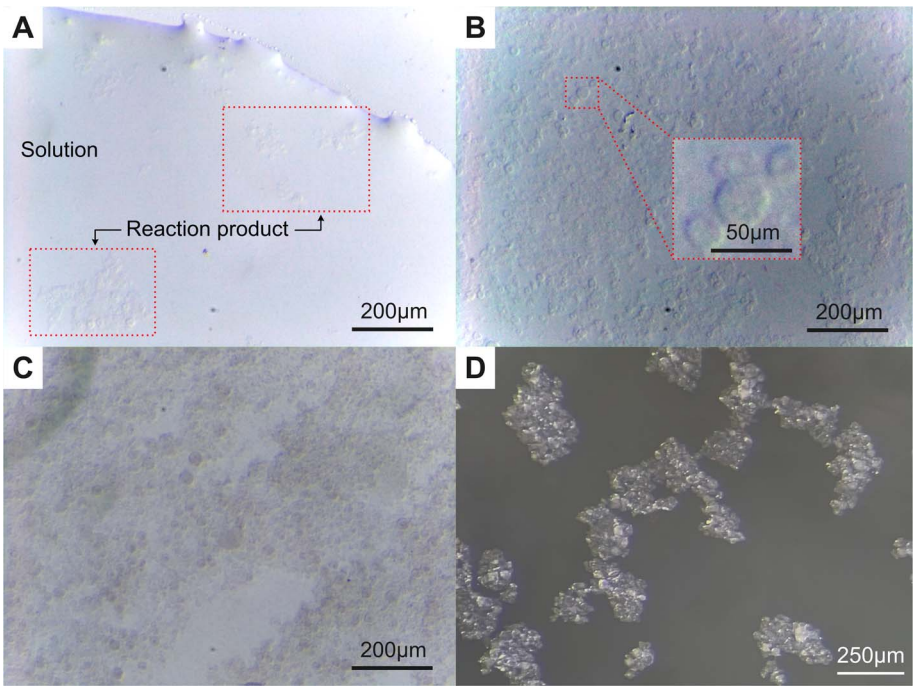

Fig. 3 Microscope imaging of soft calcium alginate microspheres suspended in bulk calcium solution after transfer to a glass microscopy slide, showing the edges (A) and centre (B) of the liquid pool. (C) Microspheres formed from precipitation of sodium alginate droplets containing carbon black ink into $CaCl_2$ solution. (D) Dark-field microscope image following precipitation of sodium alginate microdroplets containing fluorescent polystyrene particles (mean diameter 60 nm) into bulk $CaCl_2$ solution.

readily visible within the solution, Fig. 3C. Similarly, the addition of fluorescent nanoparticles rather than dye to the alginate solution produced fluorescent particles readily captured *via* dark-field microscopy, Fig. 3D.

As an initial demonstration of *in situ* chemical synthesis within the microspheres, we carried out the procedure with sodium ferrocyanide $Na_4[Fe(CN)_6]$ added to the alginate solution and along with a ferric salt ($FeCl_3$ or $Fe(NO_3)_3$) added to the bulk $CaCl_2$ solution. The hypothesis was that simultaneous diffusion of Fe^{3+} and Ca^{2+} cations from bulk solution into the microspheres would cause Prussian blue formation *via* the reaction of Fe^{3+} and $[Fe(CN)_6]^{4-}$, with concomitant cross-

linking of alginate by Ca^{2+}. In line with this hypothesis, Prussian blue pigment particles trapped within the cross-linked alginate matrix were observed *via* optical microscopy as blue droplets with no noticeable leakage of the pigment into the bulk solution, Fig. 4A.

Compared to bulk synthesis, the aerosol medium introduces a host of new experimental variables, including reactor dimensions and the timing of aerosol release, with implications for the resultant microsphere population. Subsequent optimisation experiments sought to fine-tune the properties of the alginate microdroplets *via* these variables, in addition to identifying a range of parameters producing a robust and consistent outcome. To this end, we explored the relationship between the number and duration of aerosol release module activations (pulses) single pulses on the size and number of total calcium alginate microdroplets. Particle counts and diameters were measured after 75, 150, 300, and 600 actuator pulses, each at both 25 and 50 ms durations. For each combination of parameters, microscope images of 10 random 1 mm^2 locations were captured and the boundaries of each droplet mapped *via* a machine vision model, Fig. 4B.[51] With droplet location and area tabulated, droplet diameter (assuming a circular boundary; $A = \pi d^2/4$) and count distributions can be tabulated.

While the number of calcium alginate particles shows a general increase with pulse number, Fig. 4C, particle diameter does not show the same pronounced dependence on the number or duration of activations, Fig. 4D. A comprehensive statistical analysis of particle size distributions across pulse count/duration combinations is provided in the ESI,† including 95% confidence intervals for differences in mean particle diameters. Beyond a microsphere density of *ca.* 400 mm^{-2} we noted that overlap between individual microspheres led to the formation of a continuous film on the surface.

Aerosol–aerosol reactivity

In contrast to the aerosol–bulk method, aerosol–aerosol reactivity is not dependent on precipitation of microdroplets. To test the viability of this route and demonstrate the possibility of

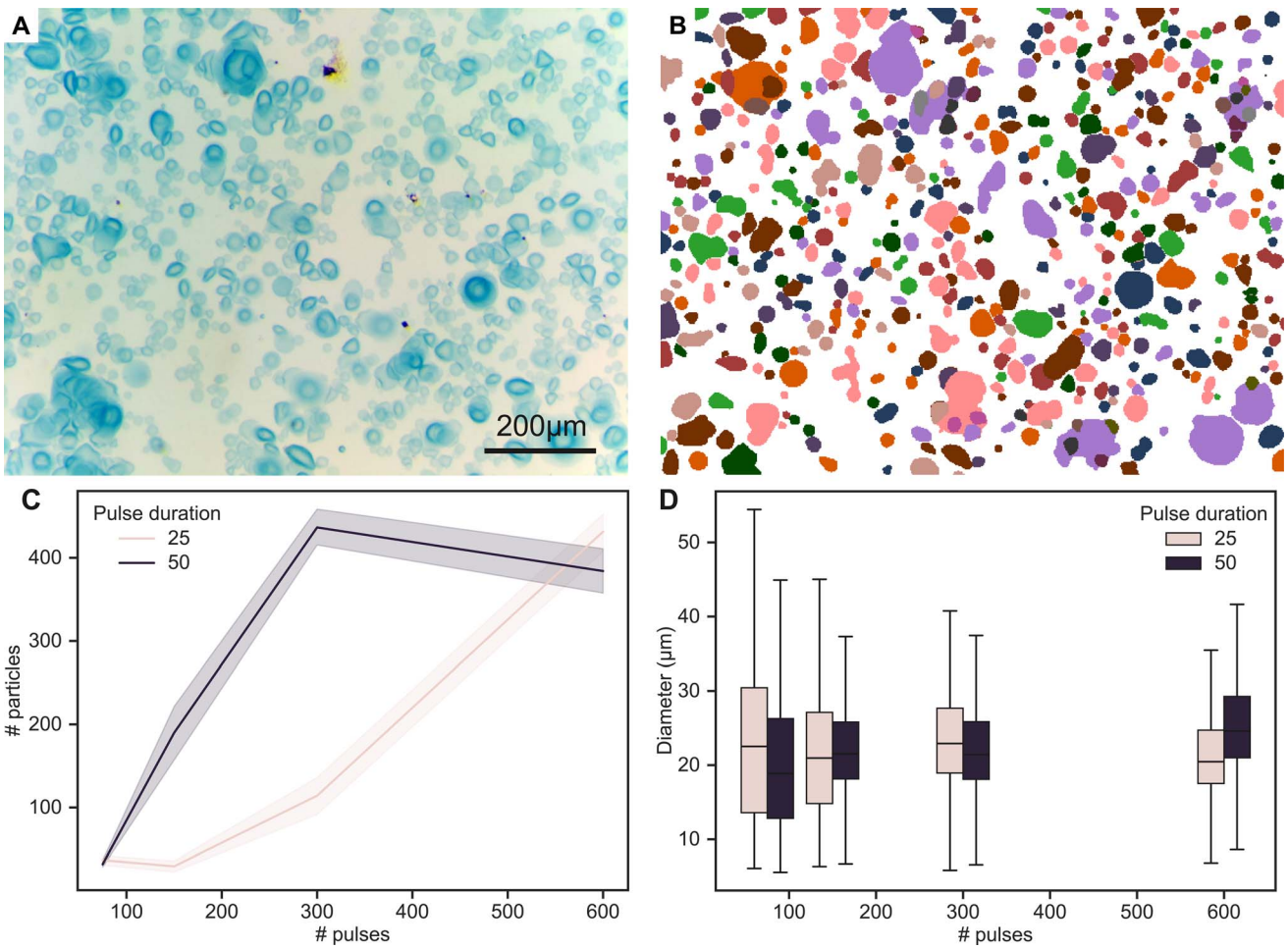

Fig. 4 *In situ* synthesis of Prussian blue in microspheres through the reaction of sodium alginate droplets containing $Na_4[Fe(CN)_6]$ with $CaCl_2$ bulk solution containing Fe^{3+}. (A) Microscope picture of product microspheres showing encapsulation of Prussian blue particles formed *in situ*. (B) Automated extraction of count and diameter data *via* segmentation of microscope image in part A using a machine vision model. Colours are arbitrarily assigned to differentiate between overlapping regions. Particle count and diameter statistics of calcium alginate particles as a function of the number and duration of aerosol release pulses. (C) Variation of particle count, the shaded area corresponding to 95% confidence interval for mean particle count determined *via* bootstrap. (D) Box plot depicting the variation of particle diameter.

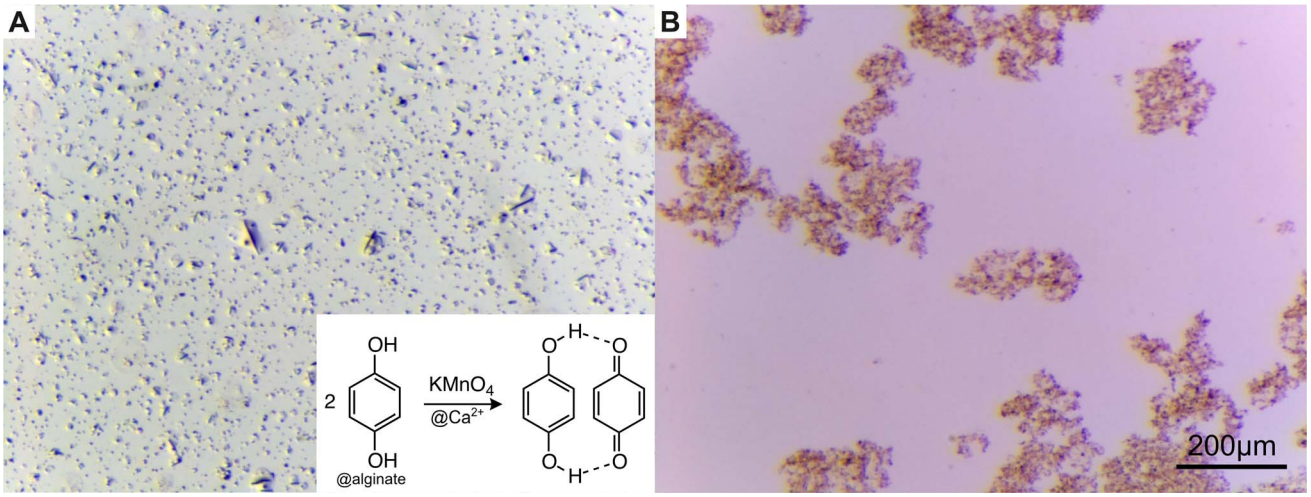

Fig. 5 Airborne *in situ* synthesis of quinhydrone (black particles) *via* the reaction between hydroquinone added to sodium alginate microdroplets and potassium permanganate added to calcium chloride microdroplets, collected on glass (A) and water (B).

using organic reagents within the droplets, we used a reactor with two aerosol sources — one containing alginate and benzene-1,4-diol (hydroquinone) and the other containing calcium chloride and potassium permanganate — directed at one another. Optical microscopy of sample collected on a glass slide, Fig. 5A confirmed *in situ* formation of black quinhydrone *via* permanganate oxidation of hydroquinone.

We were able to confirm the formation of quinhydrone within airborne microdroplets rather than on the glass substrate by collecting the droplets in a Petri dish filled with water, Fig. 5B. In line with the formation of microspheres through direct microdroplet collisions rather than precipitation, the vast majority of particles are under 10 μm in diameter (see ESI† for quantitative comparison). Once the microspheres are surrounded with water, any residual permanganate within is quickly leached into the surrounding water, resulting in the faint purple hue visible in, Fig. 5B.

More complex droplet compositions and responsive behaviour

Exploring the scope of including additional components within the micro-reactors, the incorporation of solid metal oxides was investigated to prove feasibility of access to inhomogeneous catalysis within a microsphere. Adding powdered magnetite (Fe_3O_4) to the solution of alginate and ferrocyanide used in Prussian blue synthesis, optical microscopy confirmed inclusion of small black Fe_3O_4 particles within the final blue microspheres, Fig. 6A. We did not observe any reaction to external magnetic fields in preliminary tests on these particles but envision optimising the type of included magnetic particle and loading ratio to produce a stronger magnetic response.

We also investigated the responsiveness of the soft microspheres to their chemical environment. As the structure is held together by calcium cross-linking of alginate anions, it was

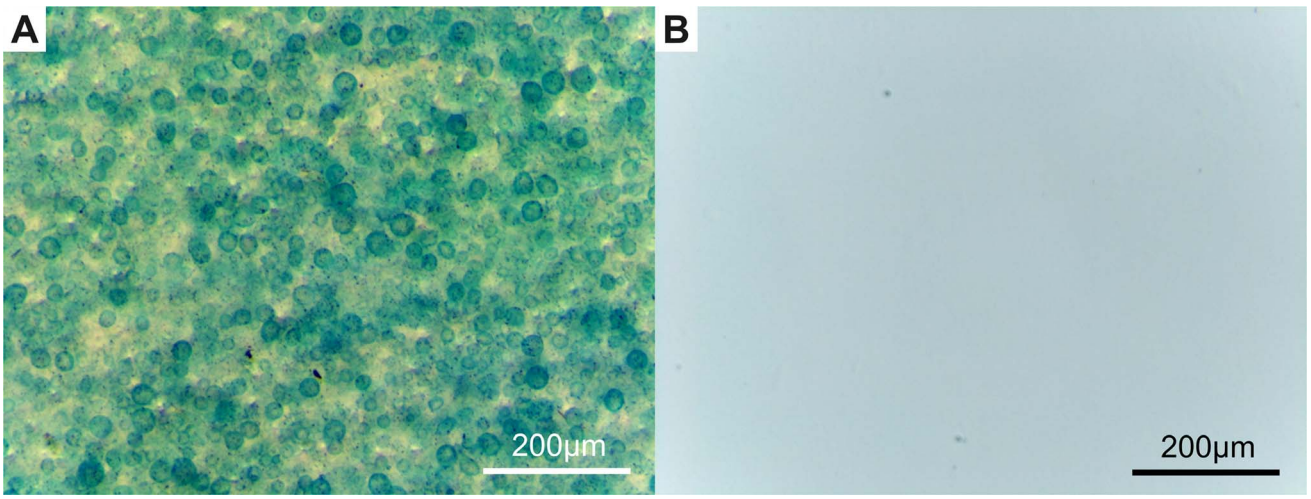

Fig. 6 Microscope imaging of soft calcium alginate microspheres after adding Fe_3O_4 in the alginate solution. (A) Results of reaction between $Na_4[Fe(CN)_6]$ and Fe_3O_4-containing sodium alginate microdroplets and $CaCl_2$ bulk solution containing Fe^{3+}. (B) EDTA-triggered disintegration of soft calcium alginate microspheres in part A with release of Prussian blue and magnetite payloads.

envisioned that addition of a calcium sequestering agent such as ethylenediaminetetracetate (EDTA) would reverse the process. As expected, addition of EDTA to the product in Fig. 6B, containing both Fe_3O_4 and Prussian blue payloads, caused rapid dissolution of the microdroplets with payload dispersal, in line with literature experiments using similar reagents, such as phosphate or citrate.[25,52]

The influence of these hydrogel microreactors on the chemical reactivity of their payload can be put in context referring back to Fig. 1A. Specifically, reactions taking place over minutes will be dominated by reagent diffusion in and out of the particle, resulting in virtually homogenous reactivity. Faster reactions primarily take place at the microdroplet boundary, with insoluble or large products trapped in the hydrogel matrix, as in the case of Prussian blue synthesis.

Methods

When comparing synthesis in the aerosol phase to bulk synthesis techniques, there is a gap in the range of available engineering controls to ensure consistent experimental outcomes. Aerosol particles are constantly evolving, and subject to rapid evaporation, ripening, coagulation (*i.e.* merging *via* collision), and precipitation, amplifying the need for robust, standardised controls.[53] To translate our qualitative reaction schemes to procedure for reliable and reproducible execution, we devised a programmable module for aerosol release, along with a modular aerosol reaction chamber.

Aerosol generation

Aerosol microdroplets can be generated using a range of methods, including pneumatic jet and ultrasonic wave nebulisers,[54] as well as electrospray, each characterised by size distribution, particle count, and charge. We used ultrasonic vibrating mesh atomisers (VMA)[55] in this work, owing to their broad chemical compatibility, cost efficiency, and amenability to digital control *via* our simple programmable driver circuit. In operation, the VMA forces liquid through a mesh of micron-sized holes laser-drilled into a small metal disc that vibrates under the influence of a piezoelectric actuator. This mechanism of action leads to a direct relationship between the droplet size and the VMA's hole diameter.[56–58]

Programmable aerosol release

Programmable generation of aerosol particles was achieved using a custom reagent module. The reagent solution is placed in a vial with the capillary action of a cotton wick carrying the solution to a piezoelectric actuator integrated into the bottle cap. Activating the actuator near its resonant frequency causes atomisation of the solution into a jet of microdroplets.[59–61]

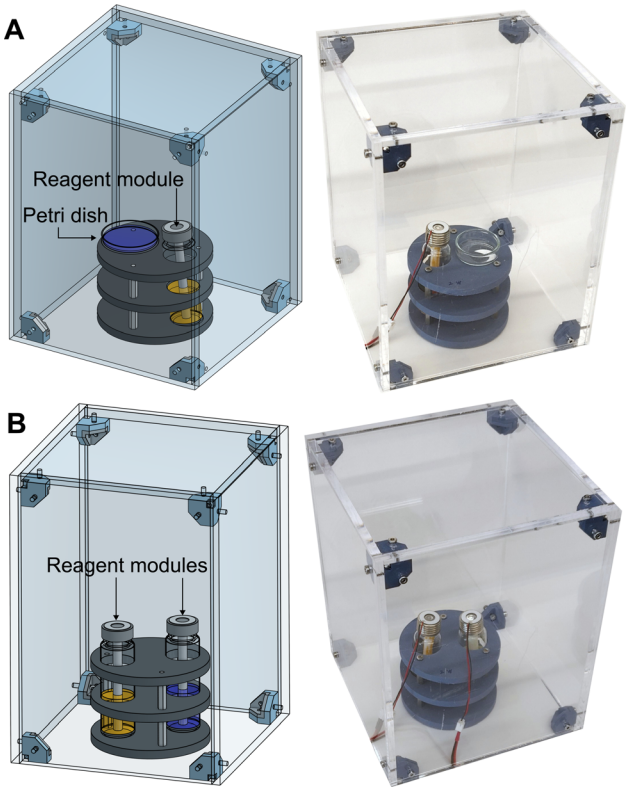

Fig. 8 Design of aerosol reactor for hydrogel particle formation *via* aerosol–bulk (A) and aerosol–aerosol (B) interaction.

In order to enable precise and reproducible dosing of alginate within the reaction chamber we created a programmable interface called CtrlAer to drive the piezoelectric actuator integrated within the reagent module using software commands, enabling coordinated release of reactants, Fig. 7A. Conceptually, CtrlAer programs describe a parallel set of state machines, one per reagent module. Each state machine can transition between an active (ON) state, in which the controller drives the corresponding piezoelectric actuator, and inactive (OFF), where no signal is sent to the actuator. State transitions are executed in lockstep driving all reagent modules synchronously. The implementation is based on the Raspberry Pi RP2040 microcontroller and takes advantage of the chip's programmable input/output functionality. User programs are specified in

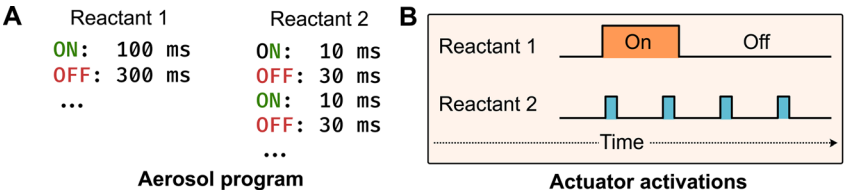

Fig. 7 Programming aerosol generation. (A) Reaction sequence involving simultaneous release of two reagents with specific timing and dose. (B) Visualisation of the same reaction sequence executed within the programmable aerosol reactor.

Table 1 Composition of reactants used in different experiments

Experiment (figure)	Solution A	Solution B
Fig. 3A and 2B	SA[a]	Ca^{2+} (bulk)[b]
Fig. 3C	SA + black ink	Ca^{2+} (bulk)
Fig. 4A	SA, 0.025 M $Na_4[Fe(CN)_6]$	Ca^{2+}, 0.025 M Fe^{3+}(bulk)[c]
Fig. 6A	SA, 0.01 M $Na_4[Fe(CN)_6]$, Fe_3O_4	Ca^{2+}, 0.025 M Fe^{3+}
Fig. 3D	SA, fluorescent particles	Ca^{2+} (2%)
Fig. 5	SA, 0.5% hydroquinone	6% $CaCl_2$ + 1.5% $KMnO_4$

[a] SA: Aqueous sodium alginate (0.25% w/w). [b] $CaCl_2$: Aqueous calcium chloride 1% w/w. [c] Both $FeCl_3$ and $Fe(NO_3)_3$ were tested.

a high-level embedded domain specific language (DSL)[62] based on the MicroPython[63] programming language. Following successful examples in other fields,[64] our system aims to widen access to programmatic control of aerosol particles *via* open hardware and a user-friendly programming language (see ESI† for complete listing of aerosol programs used in this work).

Modular aerosol reactor

The reactor consists of a box providing a closed environment for aerosol reactions housing a 3D printed reagent module holder, Fig. 8. To aerosol–bulk reactivity a Petri dish containing the bulk reactant was positioned adjacent to the aerosol source. Upon activation of the reagent module, microdroplets containing sodium alginate are introduced into the reactor as an aerosol, ultimately precipitating into the Ca^{2+} solution contained in the Petri dish. Upon contact with bulk calcium solution, these droplets are transformed to calcium alginate hydrogel microspheres. Product microspheres formed using this protocol are ideally suited to observation *via* optical microscopy, following manual transfer to a microscopy slide. Design specifications and technical drawings are provided within the ESI.†

Microsphere formulation

A range of chemistries can be used for hydrogel formation. This work focuses on calcium-mediated hydrogelation of alginate. Table 1 describes the composition of reagent solutions used in each experiment. In each case, two solutions called A and B were prepared. Solution A was used in conjunction with our programmable reagent module for aerosol generation, while solution B was employed in bulk or aerosolised form depending on the experiment as indicated for each table entry.

Conclusion

Classical chemical containers provide a means of confining reactivity, fully excluding it from the outside environment. The permeable micron-sized containers demonstrated here permit reagent diffusion across their cross-linked alginate interior, enabling reactions to occur inside as well as outside the container. They occupy a size regime where the interplay between diffusion and reactivity can play a significant role on the locus of reactivity, Fig. 9. Our programmable system provides reproducible access to a wide range of micron-sized permeable containers and establishes their feasibility as soft

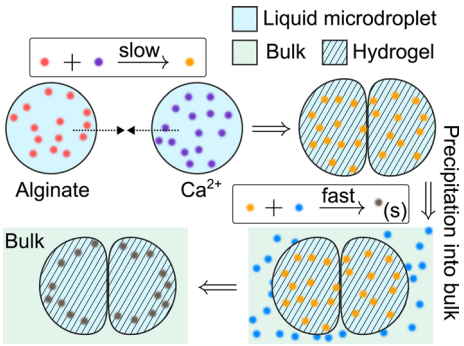

Fig. 9 Sequential reactivity of droplet payload modulated by activation and diffusion. Collision between airborne alginate and Ca^{2+} microdroplets carrying mutually reactive payloads leads to initial hydrogel formation accompanied by a slow reaction yielding an even distribution of product throughout the hydrogel matrix. Following precipitation into bulk solution, a rapid second reaction producing insoluble product results in solid particles primarily trapped within the hydrogel matrix.

chemical micro-reactors. Offering innate high throughput and amenable to large-scale parallel data collection *via* chemical imaging techniques, its development dovetails with the need for experiments offering higher data bandwidth as a substrate for digital discovery.

In principle, the same strategy used for Prussian blue synthesis could be applied to nanoparticle synthesis, following established methodology for nanoparticle preparation *via* reduction of silver or gold ions within pre-formed hydrogel matrices.[65,66] Specifically, the reduction of silver ions to form silver nanoparticles could be achieved by incorporating $AgNO_3$ in the $CaCl_2$ solution and $NaBH_4$ in the alginate solution. This approach would be compatible with our setup, as it avoids premature cross-linking of alginate by Ag^+ ions. Rapid mixing during droplet formation would initiate the reduction reaction, potentially leading to the formation of silver nanoparticles within the cross-linked alginate matrix. Other redox reactions could also be explored, such as the formation of gold nanoparticles using $HAuCl_4$ and a reducing agent like citrate or ascorbic acid. Both examples are known to occur over a timescale of hours, so only the aerosol–aerosol protocol would be applicable. There is also literature precedent for larger calcium alginate droplets used as containers for a range of other redox reactions.[67] We anticipate the fastest such reactions — those essentially complete in less than 1 s — to occur analogously in

microdroplets, while slower reactions will be preceded by homogenisation of reactants across the microdroplet boundary.

While we focused on a select few reactions to establish proof-of-concept, this methodology opens up a wide range of possibilities for future investigation. Considering the setup itself, vibrating mesh atomisers with a range of orifice sizes are available commercially, providing access to larger or smaller microdroplets. Other modes of aerosol production can also be used, including droplet-on-demand systems for a narrower particle distribution precisely controllable *via* the activation signal.[68] Other reactivity options can be pursued including nanoparticle preparation, for which there is precedent of bulk synthesis within a hydrogel matrix.[65]

Longer-term, chemical exchange between microreactors and their environment over longer time scales can serve as the basis for evolving protocells. Additionally, direct reactivity between aerosol particles holds untapped potential for synthesising reactive micro-environments with tailored composition and internal chemical dynamics. Extended setups with additional aerosol sources can unlock the programming of reaction cascades within the micro-reactors by scheduling further collisions with precise and programmable control. Concomitantly, the massive drop in reagent volume required per reactivity observation — from millilitres to picolitres — represents progress towards high-throughput experimentation with minimal generation of waste and environmental impact.

Alongside applications of these microreactors as a new medium for chemical synthesis and discovery, we expect to see continued exploration of their functionalisation, *e.g.*, loading with catalysts and daughter compartments, as well as fine-tuning of their properties by additional cross-linking steps and bespoke channels for improved control over the exchange of chemicals.

Data availability

The design and specifications of our aerosol reactor are documented within the ESI,† including access to CAD files, with the associated open-source programming system (CtrlAer) available freely at **https://github.com/MehrResearch/ureactors**. Microscope images, both for qualitative inspection and particles statistics are available *via* Zenodo at **https://zenodo.org/records/13837238**. The GitHub repository includes a Jupyter notebook for full reproduction of our particle statistics analysis starting from raw images. CAD files for all mechanical parts are freely available *via* the onshape platform at the following location: **https://cad.onshape.com/documents/67bcf186dcd4021bc9b4f106/w/bdd8e063eb0deed3427110fc/e/a9bb2837d79e4329a49a4bb1**.

Author contributions

LZ synthesised the microspheres in the lab and characterised them *via* microscopy. SHMM conceived the idea, obtained funding for the project, designed and implemented the hardware setup and CtrlAer system, and selected the chemistry used in the laboratory experiments with input from LZ. The authors jointly wrote the manuscript.

Conflicts of interest

The authors declare no conflicts of interest.

Acknowledgements

This work was supported by the Leverhulme Trust Early Career Fellowship (ECF-2021-298), the Royal Society of Chemistry Research Enablement Grant (E22-7895308996), and the University of Glasgow Lord Kelvin/Adam Smith (LKAS) Fellowship. We would like to thank Prof Mark MacLachlan (University of British Columbia), Prof Stephen Mann (University of Bristol), Dr Abhishek Sharma (University of Glasgow), and Dr Manlio Tassieri (University of Glasgow) for feedback and fruitful discussions on this manuscript. SHMM would like to thank Dr Daniel Salley for guidance on the mechanical design of the aerosol reaction chamber.

References

1 W. Kueng, E. Silber and U. Eppenberger, Quantification of cells cultured on 96-well plates, *Anal. Biochem.*, 1989, **182**(1), 16–19.
2 H. Jordan J and C. Gibb B, Molecular containers assembled through the hydrophobic effect, *Chem. Soc. Rev.*, 2015, **44**(2), 547–585.
3 M. Fujita, D. Oguro, M. Miyazawa, H. Oka, K. Yamaguchi and K. Ogura, Self-assembly of ten molecules into nanometre-sized organic host frameworks, *Nature*, 1995, **378**(6556), 469–471.
4 D. Fiedler, D. H. Leung, R. G. Bergman and K. N. Raymond, Selective Molecular Recognition, C−H Bond Activation, and Catalysis in Nanoscale Reaction Vessels, *Acc. Chem. Res.*, 2005, **38**(4), 349–358.
5 W. Liu and J. F. Stoddart, Emergent behavior in nanoconfined molecular containers, *Chem*, 2021, **7**(4), 919–947.
6 G. Bester and A. Zunger, Electric field control and optical signature of entanglement in quantum dot molecules, *Phys. Rev. B*, 2005, **72**(16), 165334.
7 V. Krishnan, S. A. Park, S. S. Shin, L. Alon, C. M. Tressler, W. Stokes, *et al.*, Wireless control of cellular function by activation of a novel protein responsive to electromagnetic fields, *Sci. Rep.*, 2018, **8**(1), 8764.
8 S. Zarra, M. Wood D, A. D. Roberts and R. J. Nitschke, Molecular containers in complex chemical systems, *Chem. Soc. Rev.*, 2015, **44**(2), 419–432.
9 P. Ballester, M. Fujita and J. Rebek, Molecular containers, *Chem. Soc. Rev.*, 2015, **44**(2), 392–393.
10 A. A. Markov, Gasdynamic and Thermal Effects of the Synthesis of Micron-Sized Particles by the Carbon Combustion Method in Straight-Flow and Three-Zone Reactors, *Fluid Dyn.*, 2022, **57**(3), 234–246.
11 S. P. Fisenko, W. N. Wang, I. Wuled Lenggoro and K. Okyuama, Evaporative cooling of micron-sized droplets in a low-pressure aerosol reactor, *Chem. Eng. Sci.*, 2006, **61**(18), 6029–6034.

12 S. Deshpande and C. Dekker, On-chip microfluidic production of cell-sized liposomes, *Nat. Protoc.*, 2018, **13**(5), 856–874.
13 P. Pattanayak, S. K. Singh, M. Gulati, S. Vishwas, B. Kapoor, D. K. Chellappan, *et al.*, Microfluidic chips: recent advances, critical strategies in design, applications and future perspectives, *Microfluid. Nanofluids*, 2021, **25**(12), 99.
14 C. Liu, C. Y. Hong and C. Y. Pan, Polymerization techniques in polymerization-induced self-assembly (PISA), *Polym. Chem.*, 2020, **11**(22), 3673–3689.
15 H. Wu, X. Du, X. Meng, D. Qiu and Y. Qiao, A three-tiered colloidosomal microreactor for continuous flow catalysis, *Nat. Commun.*, 2021, **12**(1), 6113.
16 J. Y. Kim, F. Haque, J. H. Lee, Y. J. Park, J. H. Seo, M. Mativenga, *et al.*, Practical organic electronic noses using semi-permeable polymer membranes, *Appl. Mater. Today*, 2024, **37**, 102137.
17 A. Ruhela, G. N. Kasinathan, S. N. Rath, M. Sasikala and C. S. Sharma, Electrospun freestanding hydrophobic fabric as a potential polymer semi-permeable membrane for islet encapsulation, *Mater. Sci. Eng. C*, 2021, **118**, 111409.
18 S. Banerjee, E. Gnanamani, X. Yan and R. N. Zare, Can all bulk-phase reactions be accelerated in microdroplets?, *Analyst*, 2017, **142**(9), 1399–1402.
19 A. B. Grommet, M. Feller and R. Klajn, Chemical reactivity under nanoconfinement, *Nat. Nanotechnol.*, 2020, **15**(4), 256–271.
20 L. A. Estroff, L. Addadi, S. Weiner and A. D. Hamilton, An organic hydrogel as a matrix for the growth of calcite crystals, *Org. Biomol. Chem.*, 2004, **2**(1), 137–141.
21 A. Garai, W. Shepherd, J. Huo and D. Bradshaw, Biomineral-inspired growth of metal–organic frameworks in gelatin hydrogel matrices, *J. Mater. Chem. B*, 2013, **1**(30), 3678–3684.
22 B. Amsden and N. Turner, Diffusion characteristics of calcium alginate gels, *Biotechnol. Bioeng.*, 1999, **65**(5), 605–610.
23 J. M. C. Puguan, X. Yu and H. Kim, Diffusion characteristics of different molecular weight solutes in Ca–alginate gel beads, *Colloids Surf., A*, 2015, **469**, 158–165.
24 J. Øyaas, I. Storrø, H. Svendsen and D. W. Levine, The effective diffusion coefficient and the distribution constant for small molecules in calcium-alginate gel beads, *Biotechnol. Bioeng.*, 1995, **47**(4), 492–500.
25 T. Y. Sheu and R. T. Marshall, Microentrapment of Lactobacilli in Calcium Alginate Gels, *J. Food Sci.*, 1993, **58**(3), 557–561.
26 C. Bennacef, S. Desobry-Banon, L. Probst and S. Desobry, Advances on alginate use for spherification to encapsulate biomolecules, *Food Hydrocolloids*, 2021, **118**, 106782.
27 H. Fu, Y. Liu, F. Adrià, X. Shao, W. Cai and C. Chipot, From Material Science to Avant-Garde Cuisine. The Art of Shaping Liquids into Spheres, *J. Phys. Chem. B*, 2014, **118**(40), 11747–11756.
28 J. Sun and H. Tan, Alginate-Based Biomaterials for Regenerative Medicine Applications, *Materials*, 2013, **6**(4), 1285–1309.
29 E. Perrier and J. Hart, Smart Vectorization, In *Delivery System Handbook for Personal Care and Cosmetic Products*, Elsevier, 2005, pp. 797–816, **https://linkinghub.elsevier.com/retrieve/pii/B9780815515043500420**.
30 B. Song, H. Liang, R. Sun, P. Peng, Y. Jiang and D. She, Hydrogel synthesis based on lignin/sodium alginate and application in agriculture, *Int. J. Biol. Macromol.*, 2020, **144**, 219–230.
31 S. Damiati, In Situ Microfluidic Preparation and Solidification of Alginate Microgels, *Macromol. Res.*, 2020, **28**(11), 1046–1053.
32 P. Dimitriou, J. Li, G. Tornillo, T. McCloy and D. Barrow, Droplet Microfluidics for Tumor Drug-Related Studies and Programmable Artificial Cells, *Global chall.*, 2021, **5**(7), 2000123.
33 Z. Yin, N. Gao, C. Xu, M. Li and S. Mann, Autonomic Integration in Nested Protocell Communities, *J. Am. Chem. Soc.*, 2023, **145**(27), 14727–14736.
34 Y. Xi, D. B. Frank, A. Tatas, M. Pavlovic and L. Zeininger, Multicompartment calcium alginate microreactors to reduce substrate inhibition in enzyme cascade reactions, *Soft Matter*, 2023, **19**(39), 7541–7549.
35 J. Li, W. D. Jamieson, P. Dimitriou, W. Xu, P. Rohde, B. Martinac, *et al.*, Building programmable multicompartment artificial cells incorporating remotely activated protein channels using microfluidics and acoustic levitation, *Nat. Commun.*, 2022, **13**(1), 4125.
36 Z. Yin, L. Tian, A. J. Patil, M. Li and S. Mann, Spontaneous Membranization in a Silk-Based Coacervate Protocell Model, *Angew. Chem.*, 2022, **134**(17), e202202302.
37 G. Sharma, K. Thakur, K. Raza, B. Singh and O. P. Katare, Nanostructured Lipid Carriers: A New Paradigm in Topical Delivery for Dermal and Transdermal Applications, *Crit. Rev. Ther. Drug Carrier Syst.*, 2017, **34**(4), 355–386.
38 I. M. El-Sherbiny and H. D. C. Smyth, Smart magnetically responsive hydrogel nanoparticles prepared by a novel aerosol-assisted method for biomedical and drug delivery applications, *J. Nanomater.*, 2011, **2011**, 1–13.
39 A. V. Vorontsov, A. S. Besov and V. N. Parmon, Fast purification of air from diethyl sulfide with nanosized TiO2 aerosol, *Appl. Catal. B: Environ.*, 2013, **129**, 318–324.
40 W. Jung, Y. H. Jung, P. V. Pikhitsa, J. Feng, Y. Yang, M. Kim, *et al.*, Three-dimensional nanoprinting via charged aerosol jets, *Nature*, 2021, **592**(7852), 54–59.
41 B. R. Bzdek, J. P. Reid and M. I. Cotterell, Open questions on the physical properties of aerosols, *Commun. Chem.*, 2020, **3**(1), 105.
42 J. L. Woo, D. D. Kim, A. N. Schwier, R. Li and V. F. McNeill, Aqueous aerosol SOA formation: impact on aerosol physical properties, *Faraday Discuss.*, 2013, **165**, 357.
43 U. K. Krieger, C. Marcolli and J. P. Reid, Exploring the complexity of aerosol particle properties and processes using single particle techniques, *Chem. Soc. Rev.*, 2012, **41**(19), 6631.
44 K. P. Fennelly, Particle sizes of infectious aerosols: implications for infection control, *Lancet Respir. Med.*, 2020, **8**(9), 914–924.

45 J. Norambuena-Contreras, J. Concha, L. Arteaga-Pérez and I. Gonzalez-Torre, Synthesis and Characterisation of Alginate-Based Capsules Containing Waste Cooking Oil for Asphalt Self-Healing, *Appl. Sci.*, 2022, **12**(5), 2739.

46 C. Abram, J. Shan, X. Yang, C. Yan, D. Steingart and Y. Ju, Flame Aerosol Synthesis and Electrochemical Characterization of Ni-Rich Layered Cathode Materials for Li-Ion Batteries, *ACS Appl. Energy Mater.*, 2019, **2**(2), 1319–1329.

47 R. Strobel and E. Pratsinis S, Flame aerosol synthesis of smart nanostructured materials, *J. Mater. Chem.*, 2007, **17**(45), 4743–4756.

48 W. Y. Leong, C. F. Soon, S. C. Wong and K. S. Tee, Development of an electronic aerosol system for generating microcapsules, *J. Teknol.*, 2016, **78**(5–7), 79–85.

49 D. M. Hariyadi, S. C. Y. Lin, Y. Wang, T. Bostrom, M. S. Turner, B. Bhandari, *et al.*, Diffusion loading and drug delivery characteristics of alginate gel microparticles produced by a novel impinging aerosols method, *J. Drug Targeting*, 2010, **18**(10), 831–841.

50 A. Sohail, M. S. Turner, A. Coombes, T. Bostrom and B. Bhandari, Survivability of probiotics encapsulated in alginate gel microbeads using a novel impinging aerosols method, *Int. J. Food Microbiol.*, 2011, **145**(1), 162–168.

51 A. Kirillov, E. Mintun, N. Ravi, H. Mao, C. Rolland, L. Gustafson, *et al.*, Segment Anything, In *Proceedings of the IEEE/CVF International Conference on Computer Vision*, 2023, pp. 4015–4026, **https://openaccess.thecvf.com/content/ICCV2023/html/Kirillov_Segment_Anything_ICCV_2023_paper.html**.

52 O. Murujew, R. Whitton, M. Kube, L. Fan, F. Roddick, B. Jefferson, *et al.*, Recovery and reuse of alginate in an immobilized algae reactor, *Environ. Technol.*, 2021, **42**(10), 1521–1530.

53 W. J. Dunning, Nucleation, growth, ripening and coagulation in aerosol formation, *Faraday Symp. Chem. Soc.*, 1973, **7**(0), 7–16.

54 Z. Jianhui, Y. N. Qiufeng and W. Sun, Advances in Piezoelectric Atomizers, *Trans. Nanjing Univ. Aeronaut. Astronaut.*, 2020, **37**(1), 54–69.

55 Q. Yan, J. You, W. Sun, Y. Wang, H. Wang and L. Zhang, Advances in Piezoelectric Jet and Atomization Devices, *Appl. Sci.*, 2021, **11**(11), 5093.

56 P. Sharma, M. Quazi, I. R. Vazquez and N. Jackson, Investigation of droplet size distribution for vibrating mesh atomizers, *J. Aerosol Sci.*, 2022, **166**, 106072.

57 T. Ghazanfari, A. M. A. Elhissi, Z. Ding and K. M. G. Taylor, The influence of fluid physicochemical properties on vibrating-mesh nebulization, *Int. J. Pharm.*, 2007, **339**(1), 103–111.

58 Y. Lang and J. Zhang, Influence of piezoelectric atomizer pores on ultrasonic atomization effect, In *Proceedings of the 2014 Symposium on Piezoelectricity, Acoustic Waves, and Device Applications*, 2014, pp. 287–290, **https://ieeexplore.ieee.org/document/6998582**.

59 D. Briceño-Gutierrez, V. Salinas-Barrera, Y. Vargas-Hernández, L. Gaete-Garretón and C. Zanelli-Iglesias, On the Ultrasonic Atomization of Liquids, *Phys. Procedia*, 2015, **63**, 37–41.

60 S. Yuan, Y. Zhang and Y. Gao, Faraday instability of a liquid layer in ultrasonic atomization, *Phys. Rev. Fluids*, 2022, **7**(3), 033902.

61 V. N. Khmelev, A. V. Shalunov, R. N. Golykh, V. A. Nesterov, R. S. Dorovskikh and A. V. Shalunova, Providing the Efficiency and Dispersion Characteristics of Aerosols in Ultrasonic Atomization, *J. Eng. Phys. Thermophys.*, 2017, **90**(4), 831–844.

62 M. Fowler, *Domain-specific languages*, Addison-Wesley, Upper Saddle River, N.J., 2011, p. 597, **https://www.myilibrary.com/?id=279730**.

63 D. P. George, *MicroPython – Python for microcontrollers*, 2024, **https://micropython.org/**.

64 T. Wenzel, Open hardware: From DIY trend to global transformation in access to laboratory equipment, *PLoS Biol.*, 2023, **21**(1), e3001931.

65 K. Vimala, K. Samba Sivudu, Y. Murali Mohan, B. Sreedhar and K. Mohana Raju, Controlled silver nanoparticles synthesis in semi-hydrogel networks of poly(acrylamide) and carbohydrates: A rational methodology for antibacterial application, *Carbohydr. Polym.*, 2009, **75**(3), 463–471.

66 H. A. H. Alzahrani, M. A. Buckingham, W. P. Wardley, R. D. Tilley, N. Ariotti and L. Aldous, Gold nanoparticles immobilised in a superabsorbent hydrogel matrix: facile synthesis and application for the catalytic reduction of toxic compounds, *Chem. Commun.*, 2020, **56**(8), 1263–1266.

67 M. Ducci, Redox Reactions in Sodium Alginate Beads, *World J. Chem. Educ.*, 2019, **7**(2), 40–44.

68 B. S. Vaughn, P. J. Tracey and A. J. Trevitt, Drop-on-demand microdroplet generation: a very stable platform for single-droplet experimentation, *RSC Adv.*, 2016, **6**(65), 60215–60222.